HHS Public Access

Author manuscript

Osteoarthritis Cartilage. Author manuscript; available in PMC 2017 February 01.

Published in final edited form as:

Osteoarthritis Cartilage. 2016 February ; 24(2): 335–344. doi:10.1016/j.joca.2015.08.010.

Cell and matrix response of temporomandibular cartilage to mechanical loading

Achint Utreja[1], **Nathaniel A. Dyment**[2], **Sumit Yadav**[3], **Max M. Villa**[4], **Yingcui Li**[5], **Xi Jiang**[2], **Ravindra Nanda**[3], and **David W. Rowe**[2]

[1]Department of Orthodontics and Oral Facial Genetics, Indiana University School of Dentistry, Indianapolis, IN 46202

[2]Center for Regenerative Medicine and Skeletal Development, School of Dental Medicine, University of Connecticut Health Center, Farmington, CT 06032

[3]Department of Orthodontics, School of Dental Medicine, University of Connecticut Health Center, Farmington, CT 06032

[4]Department of Materials Science and Engineering, University of Connecticut, Storrs, CT 06269

[5]Biology Department, College of Arts and Sciences, University of Hartford, West Hartford, CT 06117

Abstract

Objectives—The generation of transgenic mice expressing green fluorescent proteins (GFPs) has greatly aided our understanding of the development of connective tissues such as bone and cartilage. Perturbation of a biological system such as the temporomandibular joint (TMJ) within its adaptive remodeling capacity is particularly useful in analyzing cellular lineage progression.

Competing interests

The authors have no competing interests to disclose.

Contributions

1. Achint Utreja – conceived and designed study, collected, assembled and interpreted data, drafted and approved article
2. Nathaniel A. Dyment – conceived and designed study, collected, assembled and interpreted data, drafted and approved article
3. Sumit Yadav – conceived and designed study, interpreted data, revised and approved article
4. Max M. Villa – collected, assembled and interpreted data, revised and approved article
5. Xi Jiang – logistical support, interpreted data, revised and approved article
6. Yingcui Li – Assisted in processing and interpreting the histological images.
7. Ravindra Nanda – collected, assembled and interpreted data, revised and approved article
8. David W. Rowe – obtained funding, conceived and designed study, interpreted data, drafted and approved article

Role of funding source

All funding sources had no influence on the design, collection, or analysis of data in this study. Funding sources are USPHS R21-AR055750, R01-AR052374, T90-DE021989 (support for NAD).

The objectives of this study were to determine: (i) if GFP reporters expressed in the TMJ indicate the different stages of cell maturation in fibrocartilage and (ii) how mechanical loading affects cellular response in different regions of the cartilage.

Design/Methods—Four-week-old transgenic mice harboring combinations of fluorescent reporters (Dkk3-eGFP, Col1a1(3.6kb)-GFPcyan, Col1a1(3.6kb)-GFPtpz, Col2a1-GFPcyan, and Col10a1-RFPcherry) were used to analyze the expression pattern of transgenes in the mandibular condylar cartilage. To study the effect of TMJ loading, animals were subjected to forced mouth opening with custom springs exerting 50 grams force for 1 hour/day for 5 days. Dynamic mineralization and cellular proliferation (EdU-labeling) were assessed in loaded vs control mice.

Results—Dkk3 expression was seen in the superficial zone of the mandibular condylar cartilage, followed by Col1 in the cartilage zone, Col2 in the prehypertrophic zone, and Col10 expression hypertrophic zone at and below the tidemark. TMJ loading increased expression of the GFP reporters and EdU-labeling of cells in the cartilage, resulting in a thickness increase of all layers of the cartilage. In addition, mineral apposition increased resulting in Col10 expression by unmineralized cells above the tidemark.

Conclusion—The TMJ responded to static loading by forming thicker cartilage through adaptive remodeling.

Introduction

The temporomandibular joint (TMJ) is a complex synovial joint that allows jaw movement in all three dimensions. The components of the TMJ that enable this complex motion include the condyle of the mandible, the glenoid fossa of the temporal bone and an interposing articular disk [1]. From a biomechanical perspective, a load applied at the surface of the mandibular condylar cartilage (MCC) translates to compressive-shear loading within the cartilage covering the condyle. This results in a complex pattern of strain-induced deformation of the tissue [2], which needs to be accommodated for continued health of the joint.

Unlike most hyaline articular cartilages in the appendicular joints, the MCC is classified as fibrocartilage [3]. Histologically, the cartilage is composed of the force-absorbent, proteoglycan-rich non-mineralized portion and the rigid mineralized region that abuts the subchondral bone. The cartilage is divided into zones based on the tissue architecture, on morphology of the cells, and on expression of specific proteins by cellular subpopulations. The superficial or articular zone is composed of cells with a flattened morphology [4]. The underling cartilaginous zone is populated by round, type I collagen-synthesizing fibrochondrocytes, which transition into type II collagen-synthesizing pre-hypertrophic chondrocytes [5]. The hypertrophic zone is characterized by type X collagen producing cells that lie beneath the chondrocytic zone starting at the tidemark, and extend into the mineralized cartilage [6]. The mineralized cartilage has not received as much attention as the soft cartilage but is an integral part of this structure as it separates the underlying subchondral bone from the MCC.

Mechanical force applied to the TMJ produces a biological response that is usually seen as an adaptation to the altered environment [7]. Growth and adaptation of the MCC to

mechanical loading have been investigated in animal experimental models by posturing the mandible forward [8]. This resulted in accelerated chondrocyte differentiation and maturation [6, 8, 9]. A major drawback of this model was the inability to measure the magnitude of applied forces. Recently, Sobue et al. [10] developed a forced mouth opening model to examine the effect of TMJ loading on the MCC. The mechanical stress on the joint produced an anabolic effect as seen by increased expression of chondrocyte maturation markers and cell proliferation [10]. Overall, this mechanical loading model was non-invasive and allowed accurate measurement of the applied force. However, the changes in individual cellular subpopulations within the MCC were not elucidated as conventional histologic techniques in wildtype animals do not allow this characterization.

While the layers of the condylar cartilage have been defined by expression of a number of genes and mechanical loading can alter the growth and maturation of condylar cells, the effect of mechanical loading on the expression of these key genes is not fully defined. Therefore, the aim of this study is to analyze the impact of static loads on the expression of key genes that map to specific layers of the MCC in multi-color GFP reporter mice. We hypothesize that the loading regimen will lead to an acute response with increased expression of the various reporters that map to different regions of the cartilage, resulting in overall hypertrophy of the condyle.

Materials and Methods

GFP reporter mice

All experiments were performed under an institutionally approved IACUC protocol (100547-1015). The Dkk3-eGFP transgene (Dkk3-green) was obtained from the MMRRC repository (MMRRC:MGI:4846992) (http://www.mmrrc.org/). It was developed from a bacterial artificial chromosome (BAC) containing eGFP in the first exon of the murine Dkk3 gene.

The other GFP transgenes used in this study have been previously described. Col1a1(3.6kb)-GFPcyan (Col3.6-blue) and Col1a1(3.6kb)-GFPtpz (Col3.6-green) contain the 3.6-kb fragment of the rat type I collagen promoter that is strongly expressed in bone and weakly in fibrocartilage [11, 12]. Col2a1-GFPcyan (Col2-blue) and Col10a1-RFPchry (Col10-red) are expressed in the fibrocartilage of the TMJ within the chondrocytes and hypertrophic chondrocytes, respectively [13]. For the presented work, double-transgenic Dkk3-green x Col3.6-blue and triple-transgenic Col3.6-green x Col2-blue x Col10-red mice were generated by crossing the single transgenic mice.

TMJ mechanical loading model

The forced mouth opening model described by Sobue et al. [10] was used to analyze the effect of mechanical loading on the TMJ. Four-week-old dual transgenic mice (Dkk3-eGFP x Col3.6-cyan) were equally divided into loaded and control groups. Animals in both groups (n=6/group) received irradiated pellet chow and were anesthetized daily for the duration of the loading process with an intraperitoneal (IP) injection of ketamine/xylazine (87mg/kg/13mg/kg). A custom-made spring fabricated from 0.017″ × 0.025″ β-titanium (CNA) wire

was used to deliver a force of 50 grams at maximal mouth opening. The TMJ of the animals in the loaded group was subjected to mechanical loading by forcefully opening the mouth for 1 hour/day for 5 days. The animals in the control group were anesthetized but did not undergo loading.

Injection of fluorescent dyes to measure mineral apposition of condylar cartilage

Mineralization labels including alizarin complexone (AC) (10 mg/kg), demeclocycline hydrochloride (30 mg/kg) and calcein (30 mg/kg) (Sigma Aldrich, St. Louis, MO) were injected IP in the mice. AC was injected 24 hours prior to sacrificing the animals in the single label experiments. For the double fluorescent labeling experiments, calcein was injected on day 3 of loading and demeclocycline 1 day prior to sacrifice to observe the dynamic process of mineral apposition.

Mandibular condyle dissection

The mandibular condyle was isolated, dissected and fixed in 10% formalin for 3 days. After 3 days of fixation, the tissues were washed in PBS and placed in 30% sucrose (in PBS) overnight. The following day, the mandibular condyles were removed from the 30% sucrose and placed in cryomolds (Thermo Fisher Scientific Inc., Waltham, MA). Details of the dissection and sectioning of the condyles can be found in the supplemental materials.

EdU labeling and staining

Proliferating cells were labeled with EdU (5-ethynyl-2′-deoxyuridine) (Life Technologies, Grand Island, NY), a modified nucleoside that is incorporated during DNA synthesis [14]. EdU (30 mg/kg) was injected IP in the mice 24 hours prior to sacrificing the animals. The staining procedure was carried out on histological sections with the Click-iT EdU Alexa Fluor 647 Imaging Kit (Life Technologies, Grand Island, NY) according to the manufacturer's instructions.

Microscopy and imaging

The sagittal and frontal histologic sections were first imaged for fluorescent signals, details of which can be found in the supplemental methods. The reader is encouraged to download the high-resolution files from the journal web-link. In addition, the image stacks that were used to generate figures 1, 4 and 5 can be accessed at http://ucsci.uchc.edu/achint/.

After the fluorescent images were collected, the section was stained with Mayer's modified hematoxylin (Poly Scientific R&D Corp., Bay Shore, NY, USA) and eosin Y (Thermo Fisher Scientific, Waltham, MA, USA) or toluidine blue (TB), a metachromatic dye that stains nucleic acids blue and polysaccharides purple.

Image analysis and quantification

Changes in total cartilage area, total cells, number of EdU-labeled cells, Dkk3-green expression, Col3.6-blue expression, toluidine blue stained area, Col10-red expression, and mineralized cartilage area were all quantified from serial frontal sections. Details of the quantification can be found in the supplemental methods.

Two-photon imaging

Freshly dissected mandibular condyles were cleaned of soft tissues and placed upright in a well of paraffin wax. This assembly was placed under the objective lens of a two-photon microscope (Ultima IV; Prairie Technologies, Middleton, WI). The condyle was imaged with a water immersion objective (XLUMPlanFL 20x/0.95W; Olympus, Center Valley, PA) in phosphate-buffered saline (PBS). All motorized movements of the slide stage were programmed and controlled by the acquisition software (Prairie Viewer; Prairie Technologies, Middleton, WI). The laser was tuned to 900 nm and the emission of the fluorophores and second harmonic generation signal for collagen were acquired in the following bandpass filters: 435–485 nm (SHG, CFP), 500–550 nm (CFP, eGFP, GFPTpz), and 570–620 nm (CFP, eGFP, GFPTpz, mcherry). After the completion of each experiment, z-stacks were reconstructed in three dimensions using the 3D viewer plugin [15] for Fiji [16].

Statistics

Serial frontal sections (4–6/animal) were used for image quantification by outlining the unmineralized and mineralized condylar cartilage areas. The values from the sections were averaged to provide a single value for each biological replicate (n=12 for Dkk3-green x Col3.6-blue and n=6 for Col3.6-green x Col2-blue x Col10-red mice). Differences between the loaded and control groups for all image analysis parameters were analyzed via independent samples t-test (significance level set to $p < 0.05$) in the SPSS Statistics 20 software (IBM Corporation, Armonk, NY, USA).

Results

A preliminary tissue survey was carried out to examine the expression of the Dkk3-transgene in the reporter mouse. Expression was seen in ligaments, tendons, articular cartilage, and menisci of the knee (Fig. S1).

A low power sagittal cryosection of the mandibular condyle from a Dkk3-green x Col3.6-blue mouse is presented in Fig. 1(A–C) to illustrate the registration of the fluorescent signals to accumulated mineral at the tidemark and H&E stained section. The condylar bone that underlies the MCC shows a very strong Col3.6-blue signal overlying a uniform AC red mineralization line (arrow; panel A) that lies on mineralized bone surface (panel B) surrounding the bone marrow spaces (panel C). On the surface of overlying MCC are Dkk3-green cells while relatively faint Col3.6-blue cells reside underneath the Dkk3 layer. The boxed region of the MCC is presented at a higher magnification. [Fig. 1(A1–C2)].

Expression pattern of Dkk3 and Col3.6 within layers of the condylar cartilage

Dkk3-green and Col3.6-blue are expressed in separate but overlapping cell populations [Fig 1. (A1 vs A2)]. Dkk3-green expression is strongest in the superficial zone and gradually fades with depth. Also note that the entire articular surface is not covered with Dkk3-green cells leaving gaps (Fig. 1, arrows in C1) that exhibit no GFP signal. Col3.6-blue expression is seen as a distinct layer that begins within the Dkk3-green zone and extends down to the tidemark. The merged image [Fig. 1(A3)] reveals a population of double positive cells (cyan

in color) in the transition between the Dkk3-green and Col3.6-blue cell layers. When the GFP signals are aligned to H&E-stained image [Fig. 1(C1)], the Dkk3-green cells map to the flattened cells of the articular zone while the Col3.6-blue cells co-localize with the cartilaginous cells but do not extend to hypertrophic cells in the deeper layers.

The relation of transgene expression to mineralization

An irregular AC mineralization line that is above the underlying bone identifies the tidemark, which separates unmineralized and mineralizing cartilage of the MCC [Fig. 1(A1), arrow]. This mineralization line is within the extracellular matrix between hypertrophic cells of the deeper layers [Fig. 1(A3, C1)]. The label extends across the length of the condyle and the intensity is not uniform, suggesting that the mineral apposition rate of cartilage has regional variation.

Regional variations in Dkk3 and Col3.6 expression in the MCC

The irregular surface expression of the Dkk3-green reporter seen in Fig. 1 was investigated further using two-photon microscopy. The scanned composite image of the entire condylar surface showed an irregular pattern of Dkk3-green (Fig. 2A) that was distributed as patches of green superficial cells. A sagittal slice of the MCC (Fig. 2B) showed Dkk3-green cells on the surface, Col3.6-blue cells just underneath the surface and cells expressing both Dkk3-green and Col3.6-blue at the interface between these layers. The Dkk3-green cells were primarily seen on the surface (Fig. 2B1) and faded away by a depth of 30μm (Fig. 2B4). This suggested that there were clusters of Dkk3-positive as well as negative cells in the articular zone. The two-photon imaging demonstrated significant variation in the regional intensity of Dkk3-green expression with a higher number of cells with stronger expression associated with the anterior region of the cartilage. It also revealed a continuation of strong and dense Dkk3-green cells over the medial side of the cartilage, a region not frequently examined in experimental studies.

To better define the medial to lateral distribution of the Dkk3-green cells in the MCC that was identified by the two-photon images, serial frontal cryosections of the condyle were imaged. Representative sections from the posterior, middle and anterior regions (Fig. 3, columns 1–5) demonstrate large variation in the shape of the condyle and thickness of the MCC (Fig. 3, rows A and E). The area of non-mineralized cartilage increases from the posterior to the anterior regions (Fig. 3E) with values of 0.04±0.002 (Fig. 3E1), 0.07±0.002 (Fig. 3E2), 0.10±0.005 (Fig. 3E3), 0.14±0.001 (Fig. 3E4), 0.19±0.006 mm^2 (Fig. 3E5) (mean±SEM).

Bone mineralization labels and the expression of fluorescent reporters in the deeper layers of the MCC

The relationship of the GFP labeled cells in the deeper layers of the MCC was examined in a Col3.6-green x Col2-blue x Col10-red triple transgenic reporter mouse (Fig. 5A) that had received an injection of demeclocycline one day prior to sacrifice (Fig. 5B). The higher power images from the ROI box in panel A rebuild the GFP cell layers starting with Col3.6-green (Fig. 5D), Col2-blue (Fig. 5E) and ColX-red (Fig. 5F). While most of the cells exhibit a single color, dual color cells (Col3.6-green/Col2-blue and Col2-blue/ColX-red) can be

identified within the transitional layers (Fig. 5C). The organization of the mineralized fibrocartilage shows that the tidemark (line in Fig. 5C–F) localizes to the zone of cells with a hypertrophic morphology that express the Col2-blue (panel E) and ColX-red reporters (Fig. 5F). Overall, the transition of reporter colors from green->blue->red suggest a lineage progression from Col3.6-green chondrocytic cells to Col2-blue prehypertrophic cells to Col10-red hypertrophic cells with the latter being aligned with the beginning of the mineralized zone and extending into the mineralized cartilage.

Change in collagen architectures between the different reporter zones

The progression of Dkk3->Col3.6->Col2->ColX cells from the articular surface to the mineralized cartilage also correlates with a change in collagen architecture. Via two photon collagen SHG imaging, collagen fibers near the condylar surface form a basket weave with multiple layers of fibers oriented in hoops. The Dkk3 cells reside within this layer and the Col3.6 cells start to appear at ~20μm beneath the surface [Fig. 6(A2)]. At ~30μm beneath the surface, the collagen architecture begins to transition from large fibers with periodical banding [Fig. 6(B2)] to the smooth appearance of collagen within the walls surrounding the cells within the lacunae [Fig. 6(B4)]. The lacunar collagen signal is seen throughout the remaining layers of unmineralized and mineralized cartilage.

Fluorescent reporter changes due to mechanical loading of the MCC

The forced open mouth loading protocol of the TMJ was employed as a simple experimental method for altering the loading environment within the cartilage to determine how cells within the MCC responded to altered loading. Serial frontal cryosections shown in figure 3 contrast the control and loaded groups for changes in GFP expression (Fig. 3 rows A vs B), cell proliferation (Fig. 3 rows C vs D) and proteoglycan content (Fig. 3 rows E vs F). The overall area and total cell number within the MCC increased by 20–23% in the loaded group (Fig. 7B–C; $p<0.05$). However, cell density did not change. An increase in the GFP intensity was seen within the Dkk3-green articular zone in the loaded group compared to the control group (Fig. 7D, $p<0.05$). The increase was more intense in the anterior-medial regions although all regions were more prominent in the loaded group with the total Dkk3 area increasing by 40% in the loaded groups ($p<0.05$). In addition to Dkk3, the overall area of Col3.6blue cells increased by 35% (Fig. 7E; $p<0.05$).

The regional distribution of proliferating cells within the soft cartilaginous zone in the control and loaded groups was assessed in the same set of frontal sections by EdU labeling (Fig. 3, rows C vs D). A gradual increase in the number of EdU-positive proliferating cells was observed in a posterior to anterior direction, corresponding with the increase in cartilage thickness. Additionally, the EdU-labeled cells imaged on the same sections showed a similar trend with increased proliferation seen in the condylar cartilage in the loaded versus the control group (Fig. 7F).

The effect of the loading protocol on proteoglycan accumulation was visualized by TB staining (Fig. 3, E vs. F). TB staining is typically found within the deeper prehypertrophic and hypertrophic layers. Following loading, not only was the overall TB area increased in the loaded group but TB staining was found closer to the articular surface (Fig. 7H; $p<0.05$).

The TB staining demonstrated the presence of chondrocytic cells closer to the surface of the cartilage despite the increase in size of the overall cartilage (Fig. 7C) or Dkk3 area (Fig. 7D). The TB signal extended into in the mineralized cartilage zone and protruded further into the subchondral bone in the loaded group.

The response of the mineralized region of the MCC is shown in Fig. 8. The mineral apposition in loaded and control animals was quantified from a double label of calcein and demeclocycline. Calcein was administered 4 days prior to sacrificing the animals whereas demeclocycline was administered 1 day prior to sacrifice. The high rate of mineralized matrix formation even of the rapidly growing control animals resulted in only partial preservation of the calcein label and a wide zone of demeclocycline label (yellow). The loaded animals demonstrated a larger area of labeling matrix relative to the control (Fig. 8D). Concomitant with the increase in mineralizing matrix, the pixel area of the ColX-red cells was greater in the loaded animals (Fig. 8C), and a proportion of these cells extended ahead of the mineralizing front in the loaded group (Fig. 8B). Overall, loading enhances the accumulation of mineralized cartilage resulting in a greater separation of the unmineralized cartilage from the subchondral bone.

Discussion

The TMJ has received significant attention as a model tissue to study cartilaginous adaptation to mechanical loading. From a clinical perspective, the functional adaptation within the condyle forms the underlying basis of mandibular growth modification in Orthodontics that is used to correct various forms of skeletal jaw discrepancies [17, 18]. The basis for these changes is not adequately understood and has been attributed to generation of new bone in the condylar ramus [19, 20] or expansion of the condylar cartilage [21]. Animal studies have linked the cellular response to changes in chondrocyte biomarkers, including PTHrP [22], Sox9 [23], type II collagen [24], type X collagen and Cbfa1 [25], pointing to the importance of the MCC as the tissue within the TMJ that responds to loading by altering its pattern of growth.

Understanding how the skeleton adapts to mechanical loads is a continuing challenge to the basic biologist and bioengineer. In the case of bone, the adaption to compressive load results in the activation of the surface osteoblasts to increase appositional growth while osteoclasts reshape the bone to better adapt to the altered loading. Similarly, tendon and ligaments will alter matrix production and remodeling in response to change in mechanical loading [26]. Cells within the enthesis synthesize a proteoglycan-rich fibrocartilage to dissipate stress accumulation between the relatively compliant tendon and stiff underlying bone. The fibrocartilage mineralizes during growth, resulting in four zones: the midsubstance, unmineralized fibrocartilage, mineralized fibrocartilage, and subchondral bone. Increased mineralized fibrocartilage apposition within the enthesis can result following alteration in mechanical loading [27]. In addition to tensile loads experienced within tendons and ligaments, other fibrocartilaginous structures such as the intervertebral disc or pubic symphysis have to respond to compressive forces. Water molecules associated with glycosaminoglycan side chains of proteoglycans (i.e., TB-positive region) within the cartilage matrix resist compressive loading, while the type I and II collagen fibers within the

cartilage act as a net to hold the proteoglycans in place and resist expansion of the cartilage. The increase in toluidine blue staining found in this study is likely in response to a presumable increase in compressive loads within the MCC.

Chen at al. [13] described the expression of Col3.6-green, Col2-blue and ColX-red in the deeper zones of soft cartilage. However, a marker for the superficial articular zone was not identified. Additionally, the study did not evaluate changes in unmineralized and mineralized cartilage compartments or individual cellular subpopulations within the MCC following mechanical loading. To address these gaps in knowledge, the present study was initiated from the unexpected observation that a Dkk3-green reporter was active in the superficial zone of cartilage. This non-canonical member of the Wnt family has been most fully studied in the eye where it is strongly expressed in the retinal progenitor cells [28]. Both GFP reporters and Cre-driver constructs from the Dkk3 promoter target these cells but their activity has not been investigated in other tissues. Expression of Dkk3 at the RNA level has been observed in a wide variety of other tissues [29] and it may have an anti-proliferative activity in certain types of cancer tissues [30, 31]. Its function within the Wnt pathway is still unclear with reports of both agonistic [29] and antagonistic [32] roles depending on the model system. In the epidermis it appears to play an important role in regulating the transition of proliferative basal to differentiating superficial cells [33]. We have found that the reporter is strongly expressed in articular cartilage, ligaments, the meniscus of the knee, and at tendon insertion sites (figure S1). Clearly further study will be required to comprehend these molecular pathways and the biological role of this Dkk3 population to the overall function of the condylar cartilage and other force-transmitting structures.

From a histological perspective, a transition of maturation, based on the merging of GFP reporter colors, can be appreciated from Dkk3->Col3.6->Col2->ColX expressing cells. However, the Dkk3-green cells do not appear to be the population that proliferates since the EdU labeling is localized somewhat deeper between the Dkk3/Col3.6 zones. This observation suggests that an unidentified population of tissue resident progenitor cells is responsible for the regenerative/adaptive potential of this cartilage. Upon mechanical loading, all the layers of the unmineralized cartilage increase in size and intensity of reporter expression. Although proliferation within the sub-Dkk3 zone does increase, it cannot account for the entire increase in tissue size upon mechanical loading, as cell density within the MCC does not change. Instead, the level of chondrogenic differentiation may increase in the subDkk3 regions as manifested by stronger toluidine blue staining that extends outward to the Dkk3 zone and far into the subchondral bone.

At the mineralizing front of the cartilage, ColX-red cells extend above the tidemark and the zone of mineralization is expanded toward the unmineralized cartilage so rapidly that a sharp mineralization line is no longer evident. As type X collagen is a marker of mineralized cartilage, this finding suggests that the cells above the tidemark at the time of loading mineralized in response to the applied mechanical stimulus. Overall, this indicates that the adaptation of the MCC to the loading regimen is seen as an expansion of both the unmineralized and mineralized cartilage components. These findings are consistent with previous work demonstrating an increase in both unmineralized (PTHrP, Sox9, Col2a1) and

mineralized (Col10a1) cartilage markers by qPCR following altered loading [10]. However, the current study mapped expression of cartilage maturation genes to specific layers of the condylar cartilage unlike the qPCR analysis in previous work.

This functional adaptation response to mechanical loading by the cartilage demonstrated remarkable regional variation. The serial frontal sections that we utilized showed an increase in all cell populations from the posterior to the anterior regions that was most prominent in the medial side than on the superior ridge of the cartilage. This finding has not previously been reported, and suggests that the regional responses of the condylar cartilage to mechanical loading may depend on the loading mechanism.

In conclusion, the fluorescent reporters and mineralization activity reveals a metabolically active and integrated tissue that is remodeling to meet an alteration in the mechanical forces of forced mouth opening. The reporters provide a technological tool to explore the regional cell lineage and molecular response to mechanical loading which should be helpful in understanding TMJ disease in healthy or genetically impaired mice.

Supplementary Material

Refer to Web version on PubMed Central for supplementary material.

Acknowledgments

Supported by USPHS R21-AR055750, R01-AR052374, T90-DE021989 (support for NAD).

References

1. Singh M, Detamore MS. Biomechanical properties of the mandibular condylar cartilage and their relevance to the TMJ disc. Journal of biomechanics. 2009; 42:405–417. [PubMed: 19200995]
2. Tanaka E, van Eijden T. Biomechanical behavior of the temporomandibular joint disc. Critical reviews in oral biology and medicine: an official publication of the American Association of Oral Biologists. 2003; 14:138–150.
3. Benjamin M, Ralphs JR. Biology of fibrocartilage cells. Int Rev Cytol. 2004; 233:1–45. [PubMed: 15037361]
4. Shibukawa Y, Young B, Wu C, Yamada S, Long F, Pacifici M, et al. Temporomandibular joint formation and condyle growth require Indian hedgehog signaling. Developmental dynamics: an official publication of the American Association of Anatomists. 2007; 236:426–434. [PubMed: 17191253]
5. Ochiai T, Shibukawa Y, Nagayama M, Mundy C, Yasuda T, Okabe T, et al. Indian hedgehog roles in post-natal TMJ development and organization. J Dent Res. 2010; 89:349–354. [PubMed: 20200412]
6. Shen G. The role of type X collagen in facilitating and regulating endochondral ossification of articular cartilage. Orthod Craniofac Res. 2005; 8:11–17. [PubMed: 15667640]
7. Singh M, Detamore MS. Tensile properties of the mandibular condylar cartilage. J Biomech Eng. 2008; 130:011009. [PubMed: 18298185]
8. Shen G, Hagg U, Rabie AB, Kaluarachchi K. Identification of temporal pattern of mandibular condylar growth: a molecular and biochemical experiment. Orthod Craniofac Res. 2005; 8:114–122. [PubMed: 15888124]
9. Shen G, Rabie AB, Zhao ZH, Kaluarachchi K. Forward deviation of the mandibular condyle enhances endochondral ossification of condylar cartilage indicated by increased expression of type X collagen. Arch Oral Biol. 2006; 51:315–324. [PubMed: 16199001]

10. Sobue T, Yeh WC, Chhibber A, Utreja A, Diaz-Doran V, Adams D, et al. Murine TMJ loading causes increased proliferation and chondrocyte maturation. Journal of dental research. 2011; 90:512–516. [PubMed: 21248355]
11. Kalajzic I, Kalajzic Z, Kaliterna M, Gronowicz G, Clark SH, Lichtler AC, et al. Use of type I collagen green fluorescent protein transgenes to identify subpopulations of cells at different stages of the osteoblast lineage. Journal of bone and mineral research: the official journal of the American Society for Bone and Mineral Research. 2002; 17:15–25.
12. Kalajzic Z, Liu P, Kalajzic I, Du Z, Braut A, Mina M, et al. Directing the expression of a green fluorescent protein transgene in differentiated osteoblasts: comparison between rat type I collagen and rat osteocalcin promoters. Bone. 2002; 31:654–660. [PubMed: 12531558]
13. Chen J, Utreja A, Kalajzic Z, Sobue T, Rowe D, Wadhwa S. Isolation and characterization of murine mandibular condylar cartilage cell populations. Cells, tissues, organs. 2012; 195:232–243. [PubMed: 21646777]
14. Cappella P, Gasparri F, Pulici M, Moll J. A novel method based on click chemistry, which overcomes limitations of cell cycle analysis by classical determination of BrdU incorporation, allowing multiplex antibody staining. Cytometry Part A: the journal of the International Society for Analytical Cytology. 2008; 73:626–636. [PubMed: 18521918]
15. Schmid B, Schindelin J, Cardona A, Longair M, Heisenberg M. A high-level 3D visualization API for Java and ImageJ. BMC bioinformatics. 2010; 11:274. [PubMed: 20492697]
16. Schindelin J, Arganda-Carreras I, Frise E, Kaynig V, Longair M, Pietzsch T, et al. Fiji: an open-source platform for biological-image analysis. Nature methods. 2012; 9:676–682. [PubMed: 22743772]
17. Chu FT, Tang GH, Hu Z, Qian YF, Shen G. Mandibular functional positioning only in vertical dimension contributes to condylar adaptation evidenced by concomitant expressions of L-Sox5 and type II collagen. Arch Oral Biol. 2008; 53:567–574. [PubMed: 18243156]
18. Ruf S, Pancherz H. Temporomandibular joint remodeling in adolescents and young adults during Herbst treatment: A prospective longitudinal magnetic resonance imaging and cephalometric radiographic investigation. Am J Orthod Dentofacial Orthop. 1999; 115:607–618. [PubMed: 10358242]
19. Papachristou DJ, Papachroni KK, Papavassiliou GA, Pirttiniemi P, Gorgoulis VG, Piperi C, et al. Functional alterations in mechanical loading of condylar cartilage induces changes in the bony subcondylar region. Arch Oral Biol. 2009; 54:1035–1045. [PubMed: 19775676]
20. Tang GH, Rabie AB. Runx2 regulates endochondral ossification in condyle during mandibular advancement. J Dent Res. 2005; 84:166–171. [PubMed: 15668335]
21. McNamara JA, Peterson JE, Pancherz H. Histologic changes associated with the Herbst appliance in adult rhesus monkeys (Macaca mulatta). Semin Orthod. 2003; 9:26–40.
22. Rabie AB, Tang GH, Xiong H, Hagg U. PTHrP regulates chondrocyte maturation in condylar cartilage. J Dent Res. 2003; 82:627–631. [PubMed: 12885848]
23. Rabie AB, She TT, Hagg U. Functional appliance therapy accelerates and enhances condylar growth. Am J Orthod Dentofacial Orthop. 2003; 123:40–48. [PubMed: 12532062]
24. Rabie AB, Xiong H, Hagg U. Forward mandibular positioning enhances condylar adaptation in adult rats. European journal of orthodontics. 2004; 26:353–358. [PubMed: 15366378]
25. Van Lam S, Rabie AB. Mechanical strain induces Cbfa1 and type X collagen expression in mandibular condyle. Frontiers in bioscience: a journal and virtual library. 2005; 10:2966–2971. [PubMed: 15970550]
26. Kjaer M. Role of extracellular matrix in adaptation of tendon and skeletal muscle to mechanical loading. Physiol Rev. 2004; 84:649–698. [PubMed: 15044685]
27. Dyment NA, Hagiwara Y, Jiang X, Huang J, Adams DJ, Rowe DW. Response of knee fibrocartilage to joint destabilization. Osteoarthritis Cartilage. 2015
28. Nakamura RE, Hunter DD, Yi H, Brunken WJ, Hackam AS. Identification of two novel activities of the Wnt signaling regulator Dickkopf 3 and characterization of its expression in the mouse retina. BMC cell biology. 2007; 8:52. [PubMed: 18093317]
29. Niehrs C. Function and biological roles of the Dickkopf family of Wnt modulators. Oncogene. 2006; 25:7469–7481. [PubMed: 17143291]

30. Dellinger TH, Planutis K, Jandial DD, Eskander RN, Martinez ME, Zi X, et al. Expression of the Wnt antagonist Dickkopf-3 is associated with prognostic clinicopathologic characteristics and impairs proliferation and invasion in endometrial cancer. Gynecol Oncol. 2012; 126:259–267. [PubMed: 22555103]
31. Yin DT, Wu W, Li M, Wang QE, Li H, Wang Y, et al. DKK3 is a potential tumor suppressor gene in papillary thyroid carcinoma. Endocr Relat Cancer. 2013; 20:507–514. [PubMed: 23702469]
32. Veeck J, Dahl E. Targeting the Wnt pathway in cancer: the emerging role of Dickkopf-3. Biochim Biophys Acta. 2012; 1825:18–28. [PubMed: 21982838]
33. Lim X, Tan SH, Koh WL, Chau RM, Yan KS, Kuo CJ, et al. Interfollicular epidermal stem cells self-renew via autocrine Wnt signaling. Science. 2013; 342:1226–1230. [PubMed: 24311688]

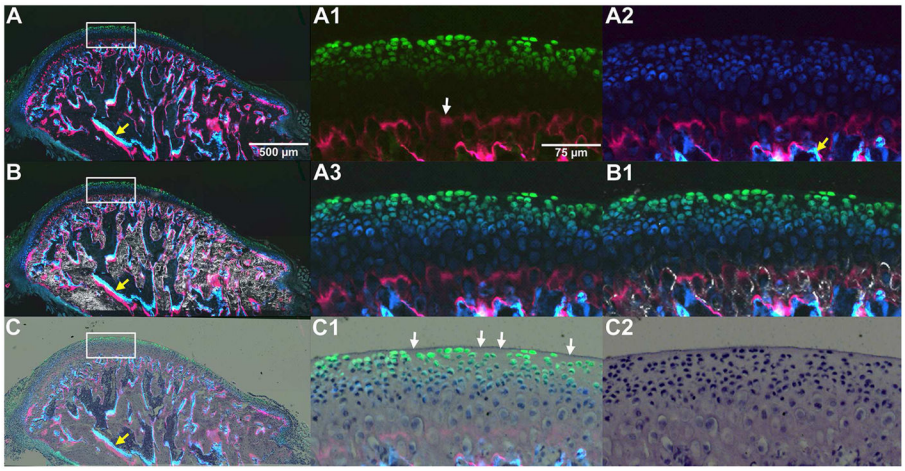

Figure 1.

Dkk3-green and Col3.6-blue expression in cells of the MCC. Scanned and tiled sagittal cryosection of the MCC showing the fluorescent (A), fluorescent and darkfield, which highlights mineralized tissue (B), and fluorescent channels with hematoxylin stained (C) images. Panels A1–C2 are higher magnification images of the box area in panels A–C. A1 shows the localization of superficial Dkk3-green cells and the irregular AC mineralization label of the tidemark (arrow in A1). In A2 the weak Col3.6-blue from the chondrocytes is not associated with the tidemark AC signal, but the strong Col3.6-blue from the subchondral osteoblasts overlie the AC label (yellow arrows in A2, & A–C). A3 is the merged image of the green and blue channels with the AC red fluorescent labels. B1 is the darkfield channel in addition to GFP reporters and AC signal from the tidemark. C1 is the fluorescent image merged with the hematoxylin stain to show the morphology of the Dkk3-green cells in the superficial zone while the Col3.6-blue cells are in the chondrocytic zone. C2 is hematoxylin alone. Note the acellular gaps between the Dkk3-green superficial cells without hematoxylin-stained nuclei (arrows in C1). Beneath the Col3.6-blue population are cells with a hypertrophic morphology (C1–2).

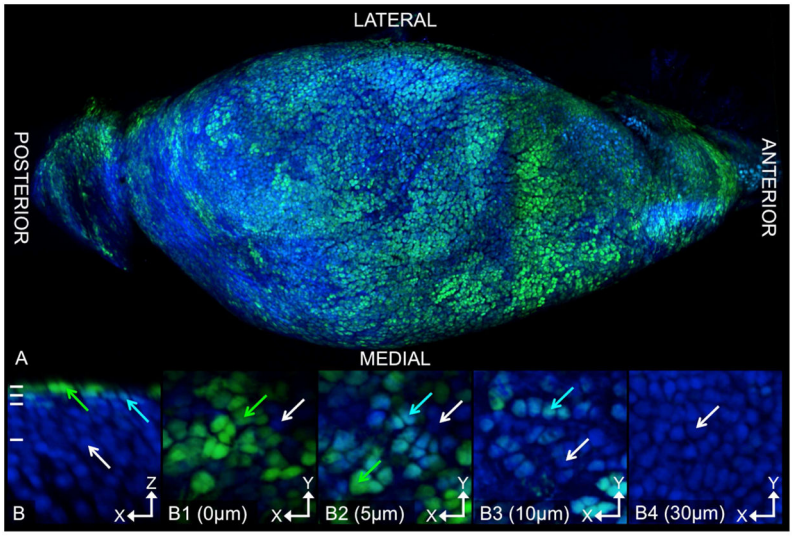

Figure 2.

Two photon image of the MCC. Supero-inferior view of the articulating surface of the mandibular cartilage from a Dkk3-green and Col3.6-blue mouse. Note the irregular, island like, clusters of Dkk3-green cells on the condylar surface. (B) Sagittal view of the MCC showing Dkk3-green cells (green arrows) on the surface, Col3.6-blue cells (white arrows) just underneath the surface and cells expressing both Dkk3-green and Col3.6-blue (cyan arrows). B1–B4 are supero-inferior slices from the surface (0μm) to a depth of 30μm (hashes in B denote position of slice in B1–4). Dkk3-green cells are primarily positioned on the condylar surface while Col3.6-blue cells are primarily positioned beneath the surface.

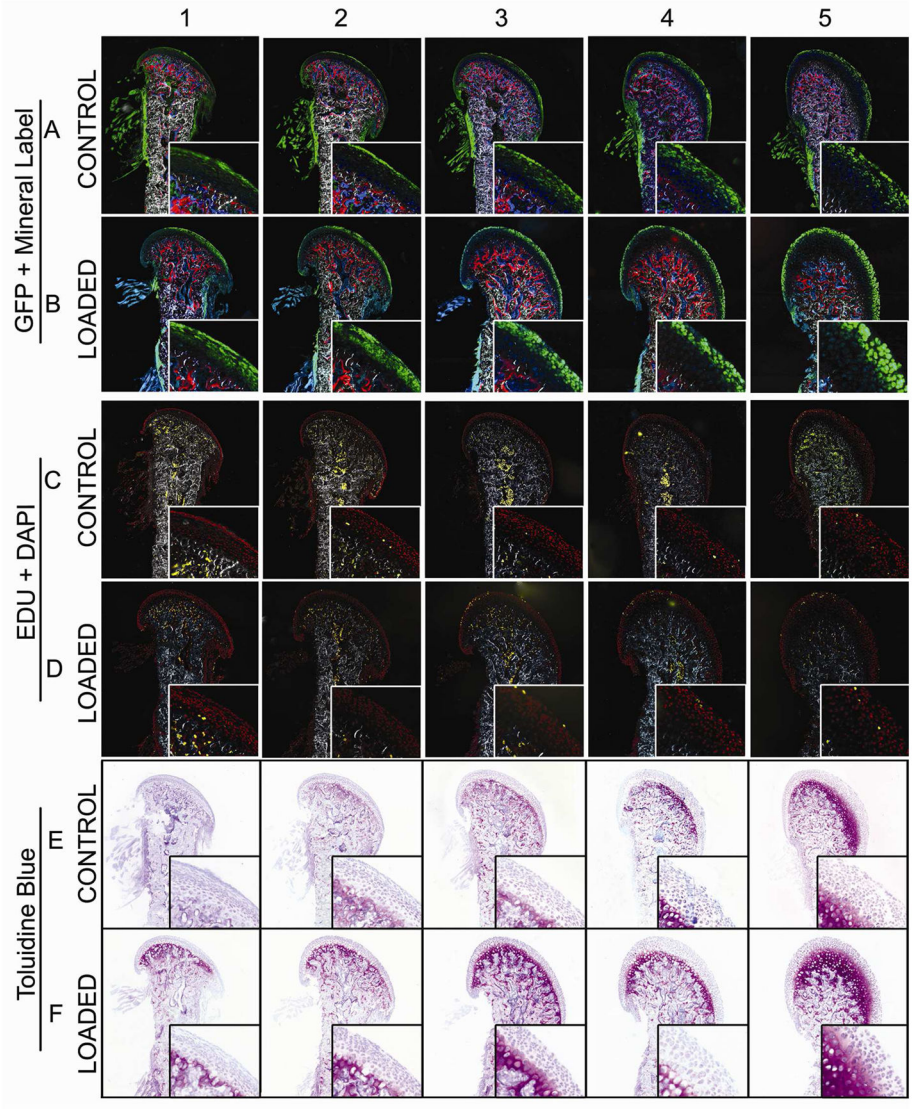

Figure 3.

Serial frontal cryosections of the MCC progressing from posterior to anterior (columns 1–5). The control group is presented in rows A, C and E to show the increasing area of unmineralized cartilage from posterior to anterior. Mechanical loading (rows B, D and F) leads to adaptive remodeling that is contrasted with the control. Dkk3-green signal increases in the loaded group (B) compared to unloaded controls (A) (see figure 7 for quantification). The EdU+DAPI staining for cell proliferation is presented in the C/D comparison. See figure 4 for more detail on the localization of the EdU relative to articular surface. The TB stain for cartilage proteoglycan accumulation is shown in the E/F comparison. The total area of TB stain is increased in the loaded group (see figure 7 for quantification).

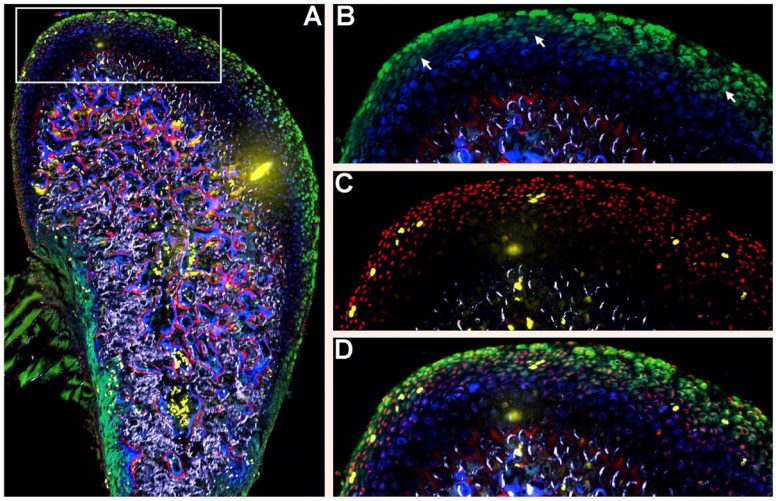

Figure 4.

Localization of the proliferating cells within the MCC of a control animal. (A) Representative enlarged image from column 4 of cryosections presented in figure 3. Panels B–D are higher magnification images of the boxed region in A. (B) Dkk3-green and Col3.6-blue expression in the superficial region of the condylar cartilage. (C) EdU-yellow and DAPI red labeling. (D) Merged image showing that the EdU-yellow expression is located in cells at the transition of Dkk3-green to Col3.6-blue cells. Arrows in B indicate EdU+ cells.

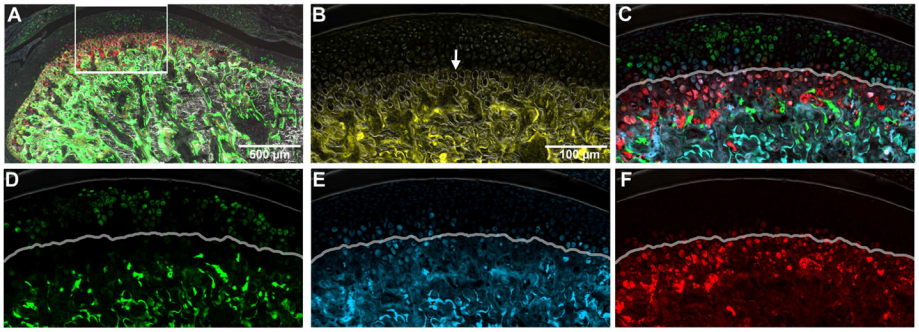

Figure 5.

Cells express more mature collagen types in deeper regions of MCC. A. Sagittal cryosection of the mandibular condylar cartilage from Col3.6-green, Col2-blue and Col10-red triple transgenic mouse. Demeclocycline (1 day before sacrifice) fluorescent label is yellow. The boxed region is presented at higher magnification in panels B–F. B) Demeclocycline label with darkfield channel demonstrating 516 the location of the tidemark (arrow). C) Composite image demonstrating the transition from Col3.6-green to Col2-blue to Col10-red cells with depth in the cartilage. Individual channels for Col3.6-green (D), Col2-blue (E), and Col10-red (F) further demonstrating the change in expression with depth. Lines in panels C–F denote the location of the tidemark.

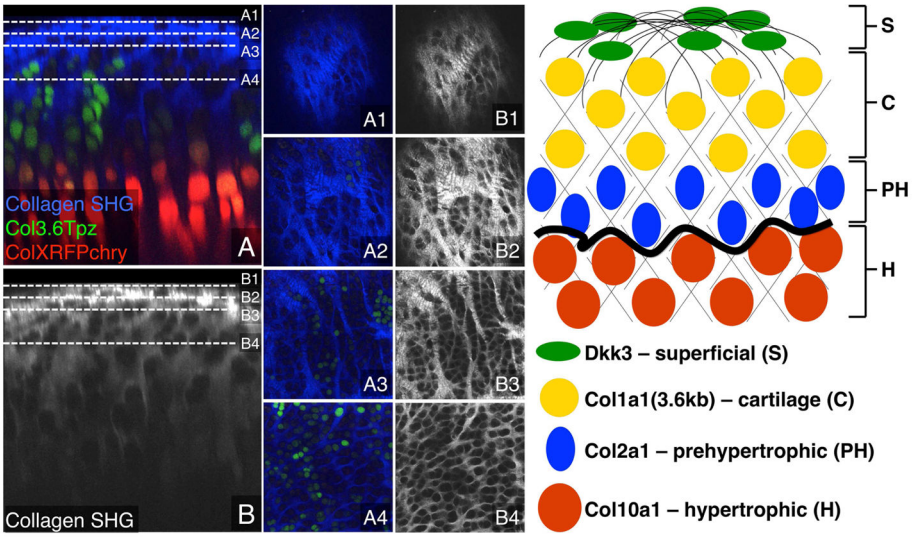

Figure 6.

Collagen organization in relation to GFP reporters within the MCC. Two photon image stack from a Col3.6-green x Col2-blue x Col10-red triple transgenic reporter mouse. Sagittal views of composite image (A) with collagen SHG (blue) with visible Col3.6-green and Col10-red cells and collagen SHG only image (B). Supero-inferior slices of the MCC at the surface (A1, B1), 20μm (A2, B2), 30μm (A3, B3), and 50μm (A4, B4) beneath the surface. The collagen organization changes from a fibrous structure with hoops of collagen at the surface (B1–2) to smooth appearance of collagen in walls within lacunae in deeper layers (B4). Schematic on right depicts location of all GFP reporters used in this study in relation to collagen organization (black lines) in MCC. S – superficial, C – chondrocytic, PH – prehypertrophic, H – hypertrophic. The 3D reconstruction of the image stack is presented as a supplemental video.

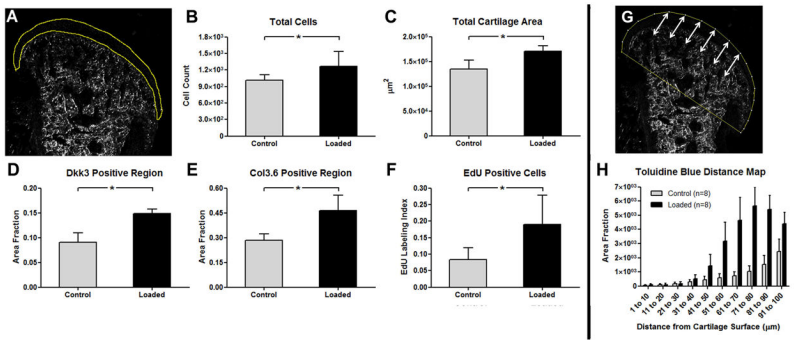

Figure 7.

Adaptive changes of the unmineralized cartilage to mechanical loading. (A) Representative outline of the unmineralized MCC on a darkfield image of a frontal cryosection demonstrating the region used to quantify panels A–F. The total number of cells (i.e., DAPI nuclei) (B), total unmineralized cartilage area (C), area fraction of unmineralized cartilage containing Dkk3 cells (D) and Col3.6 cells (E), and EdU-labeled proliferating cells (F) were all significantly higher in the loaded 539 group compared to the control group ($p<0.05$). Euclidean distance mapping of toluidine blue staining in the first 100μm from the cartilage surface (arrows in G) reveals that total proteoglycan accumulation (area under curve) not only increased but the proteoglycans also accumulated closer to the surface, with significant changes starting at 50μm (n=12; 6 sections/animal; $p<0.05$). * denote significant difference ($p < 0.05$). Error bars indicate 95% confidence interval.

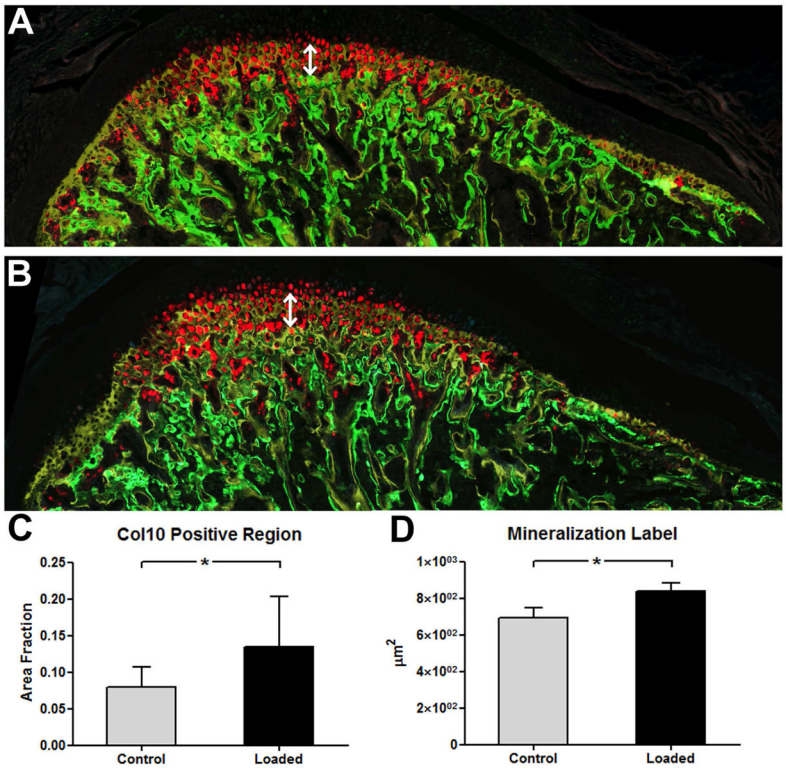

Figure 8.

Adaptive changes to mechanical loading by ColX-red hypertrophic chondrocytes within the mineralized cartilage. The mice were administered calcein (green) at 3 days of loading and demeclocycline (yellow) 1-day prior to sacrifice. The height of the forming mineralized cartilage during the period between labeling (24 hours) is shown by the double arrows in the control (A) and loaded (B) MCC. A region of interest that included the area of new mineralized cartilage apposition within the 24-hour period (defined by arrows in A and B) was used for quantification. The area fraction containing ColX-red cells is shown in panel C, while the total area undergoing active mineralization is in panel D (i.e., region of interest). Both measures are significantly increased in the TMJ loaded group (n=6, 6 sections/animal; $p<0.05$). Also note that additional ColX-red cells are present above the tidemark in the loaded animals where in the control mice these cells first appear at the tidemark. * denote significant difference ($p < 0.05$). Error bars indicate 95% confidence interval.